ELSEVIER

Journal of Neuroscience Methods 126 (2003) 195–207

JOURNAL OF NEUROSCIENCE METHODS

www.elsevier.com/locate/jneumeth

Precise placement of multiple electrodes into functionally predefined cortical locations

Michael Niessing *, Kerstin Schmidt, Wolf Singer, Ralf Galuske

Max-Planck-Institute for Brain Research, Deutschordenstraße 46, 60528 Frankfurt am Main, Germany

Received 19 November 2002; received in revised form 28 March 2003; accepted 31 March 2003

Abstract

Current research on topics such as effective connectivity, neuronal coding strategy or signal propagation in the central nervous system requires simultaneous recordings from multiple sites within functionally grouped but topologically distributed neuronal clusters. We have addressed this issue by characterization of the cortical functional architecture using optical imaging of intrinsic signals (OI) and subsequent placement of multiple, individually adjustable electrodes into pre-selected domains. In order to achieve maximum precision and flexibility for the positioning of electrodes, a plastic cylinder containing channels of an extremely high aspect ratio (density >20 channels/mm^2) was fixed above the cortex and individual channel positions were superimposed onto the functional maps of orientation columns obtained previously with OI. Subsequently, channels corresponding to the desired locations in the functional map were used as guide tubes for electrode insertion. The spatial precision of this approach was in the range of 100 μm and experiments in cat primary visual cortex revealed a close correlation between the desired and the actually recorded orientation preferences of the targeted columns. The method is applicable to all cortical areas in which OI is feasible and offers a high degree of flexibility with respect to the number and geometry of applicable probes. It is, thus, an excellent tool for studying distributed codes and interactions between multiple predefined recording sites.

Keywords: Brain mapping; Optical imaging of intrinsic signals; Feature maps; Functional architecture; Electrophysiology; Microelectrodes; Cortical domains; Electrode position

1. Introduction

The function of the brain is based on the coordinated interaction of the activity of millions of neurons. In the cerebral cortex, these neurons are embedded into a well defined architecture which is characterized by a high degree of functional and structural organization. Sensory areas usually contain a topologically ordered map of sensory surfaces and feature domains. Examples are the retinotopic (Tusa et al., 1978, 1979), somatotopic (Jones et al., 1978) and the tonotopic maps (Merzenich et al., 1975) in low level sensory areas. Allowing for some variability in details, these topological organizations are remarkably similar among animals of the same species (Tusa et al., 1979) and even across species including humans (Reppas et al., 1997; Gelnar et al., 1998; Ruben et al., 2001). Another architectonic feature of neocortex is its functional columnar organization. Columns are clusters of neurons with similar functional properties that extend perpendicular to the cortical surface through all cortical layers and exhibit a typical diameter of about 0.4 mm (cat visual cortex, Hubel and Wiesel, 1962; Hubel et al., 1977; Bonhoeffer and Grinvald, 1991). They are interconnected selectively according to their functional properties and cortical distance (Gilbert and Wiesel, 1983, 1989; Kisvarday et al., 1997; Schmidt and Löwel, 2002). Unlike the general topographic organization, the patterns of these functional sub-networks exhibit considerable inter-individual variability even between animals of the same species (e.g. Horton and Hocking, 1996), and therefore, these patterns have to be determined individually.

Current concepts and strategies in neuroscience research are based on these microstructural and con-

* Corresponding author. Tel.: +49-69-96769-240; fax: +49-69-96769-327.

E-mail address: niessing@mpih-frankfurt.mpg.de (M. Niessing).

0165-0270/03/$ - see front matter
doi:10.1016/S0165-0270(03)00091-8

nectivistic facts. Theoretical considerations and recent experimental results (for reviews see Engel et al., 2001; Salinas and Sejnowski, 2001) on the representation and processing of sensory information stress the need to search for distributed population codes by assessing temporal relations among distributed responses in order to explain how essential computations such as scene segmentation, feature binding or the flow of information are performed. To achieve these tasks, parallel electrophysiological recordings from multiple functionally defined neurons have to be accomplished. Ideally, the different recording sites should be targetable with sufficient precision to obtain responses from preselected members of the different functional micronetworks outlined above. This requires a priori knowledge about the potential recording sites and methods for the precise placement of electrodes.

As the topographic organization of functional subnetworks varies from individual to individual, the respective feature maps have to be determined prior to electrode placement and then targeting methods are required that permit precise placement of multiple electrodes according to the topology of the functional maps. Here we describe a new method that meets all of these requirements.

2. Materials and methods

2.1. The general approach for targeted recordings according to feature maps

As a general approach for the parallel electrophysiological recording from multiple predefined sites of a feature map, we chose to obtain feature maps by optical imaging of intrinsic signals (OI) and to subsequently place the electrodes by using an array of densely packed guide tubes. This array is positioned above the cortex providing a lattice of possible electrode insertion sites. In order to relate the positions of the guide tubes to positions on the feature map, a fixed reference frame is required. In our approach, this reference to cortical coordinates is established by a metal ring, the base ring, which is cemented onto the skull. This ring serves as a base for both, the optical imaging chamber (OIC) and the array of guide tubes. As the positions of the guide tubes with respect to the base ring are fixed, the only variable in this procedure to be determined is the exact position of the feature map. This part of the alignment procedure is achieved by projecting a coordinate system grid onto the cortical surface by means of a slide projector. The coordinate system is set into a defined position and rotation with respect to the base ring by adjusting the projected grid to little marks at defined positions on the OIC. An image of the projected coordinate system is taken with the optical imaging camera in exactly the same position as for the recording of the feature maps. Thus, the coordinate lines are visible in the image of the cortical surface and give all positional information about the feature map that is needed to align it with the guide tube positions. Finally a set of guide tubes is selected for insertion of electrodes according to the desired feature constellation of the neurons to record from. This procedure allows for the targeted recording of functionally specified neurons.

Before describing the procedure of electrode targeting in greater detail, we list the parts of the targeting device that is secured onto the animal's skull.

2.2. Apparatus

2.2.1. Head holder

The head holder (not shown) consists of a rippled bolt that is cemented to the skull and fastened to the stereotactic frame. The head holder has a flat design as it must not interfere with the beam of the coordinate projection device.

2.2.2. Base ring

The base ring (Fig. 1A1, 1B1, 1C), a titanium ring of 20 mm inner diameter, 30 mm outer diameter and 2 mm height. On the upper side, eight equidistantly arranged bridge-like protrusions 1 mm in height and 1 mm in width jut out of the surface, running radially from the inner to the outer ring diameter. Furthermore, the ring has a threaded hole in the middle between each protrusion at a radius of 25 mm.

2.2.3. Optical imaging chamber (OIC)

The basic concept of the OIC design has been adopted from Bonhoeffer and Grinvald (1996). However, for our purposes, the design (Fig. 1A2–8, 1B2, 1D, Fig. 2) had to be modified and new features had to be added. The resulting OIC is constructed as follows: a metal chamber (Fig. 1A2, 1B2, Fig. 2A), 9 mm in height, manufactured to fit on the base ring by having the same inner and outer diameter and at its bottom face (Fig. 1B2) the inverse geometry of the base ring's top surface (Fig. 1B1). At 2.5 mm height, the inner diameter increases from 20 to 25 mm, producing a plateau inside the chamber. A glass plate (Fig. 1A4, Fig. 2C) is placed onto the plateau with a silicone gasket ring (Fig. 1A3, Fig. 2B) in between. In order to close the chamber, a threaded metal ring (Fig. 1A5, Fig. 2D) is screwed into the OIC that presses the glass plate against the plateau and provides a tight seal. At a height of 1 mm two filling plugs (Fig. 1D indicated by an asterisk, Fig. 2H) are mounted on opposing sides of the chamber in order to fill the chamber with silicone oil for the optical recording. A metal plate with coordinate marks (Fig. 1A7, Fig. 2E) can be mounted on top of the chamber above the glass plate. These coordinate marks provide a

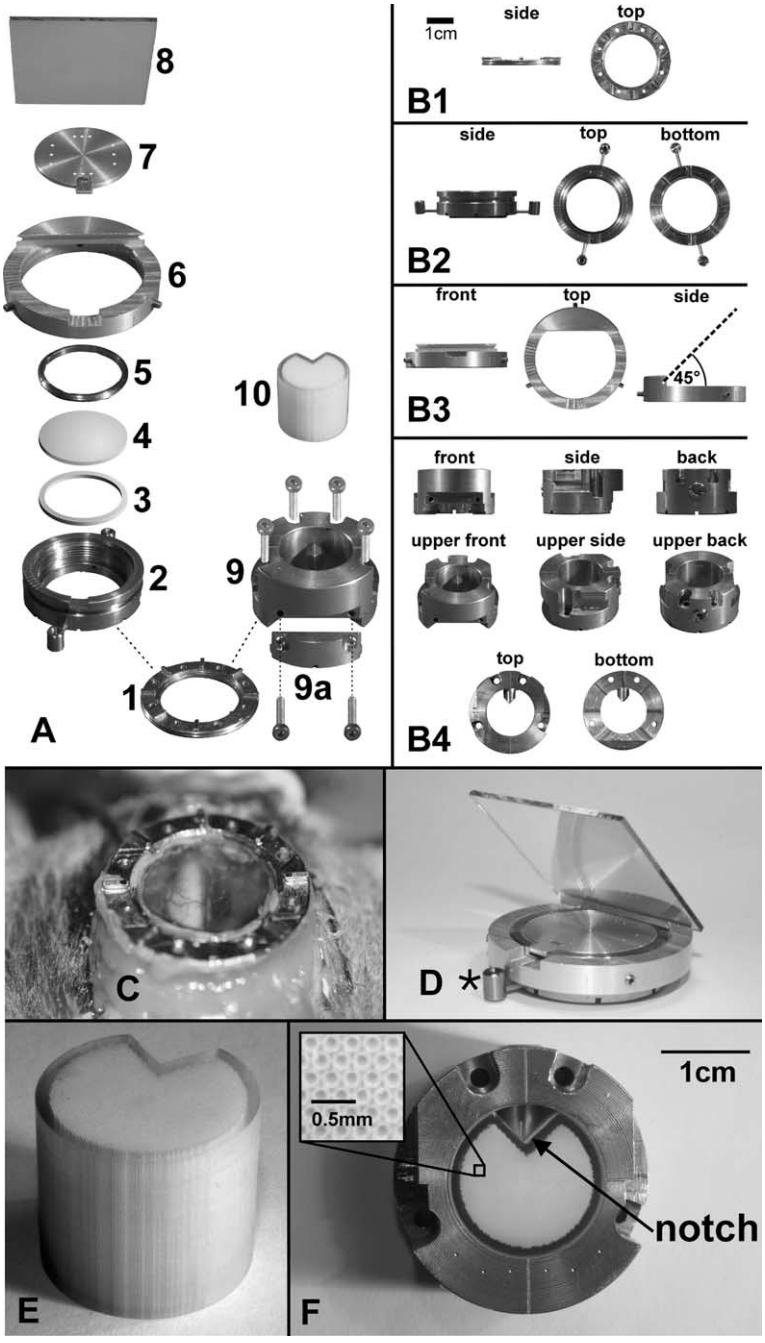

Fig. 1. Hardware items for placing electrodes according to a feature map. (A) Schematic illustration of how the OIC and the metal cylinder are pieced together from their components for mounting on the base ring (1). On the left side from the bottom to the top are shown: the basic OIC (2), silicon gasket (3), glass plate (4), threaded metal ring (5), mirror holder (6), metal plate with coordinate marks (7) and the semi-translucent mirror (8). On the right side: metal cylinder with screws (9), cover for the opening of the metal cylinder (9a) and tube grid (10). Both devices, the OIC and the tube grid holder, can be mounted onto the base ring shown at the bottom center. (B) Close-ups of the more complex components in (A). (B1) the base ring from side and above; (B2) the OIC from the side, above and from beneath; (B3) Mirror holder as seen from front, above and the left side (left to right, the dashed line indicates the mirror position); (B4) images of the metal cylinder (tube grid holder), the first row shows front, side and rear view; the images of the second row are taken from elevated front, side and rear positions. The images in the bottom row show the cylinder from above and beneath. (C) The base ring cemented onto the scull. (D) The OIC with the coordinate metal plate and the semi-translucent mirror mounted onto it. The asterisk indicates one of the two filling plugs. (D) Close-up of the tube grid. (E) The tube grid mounted into the tube grid holder and fixated by a bolt. The inset shows an enlarged area of the tube grid, thus showing the geometry of the guide tube arrangement.

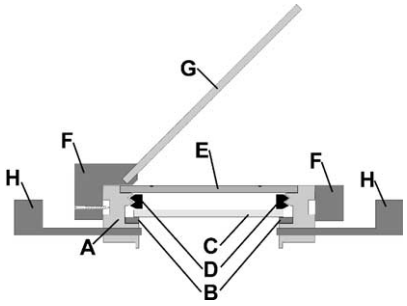

Fig. 2. True-to-scale cross-section sketch of the multi purpose OIC for recording optical data and projection of a coordinate grid onto the cortical surface. (A) The chamber. (B) Silicon gasket ring. (C) Glass plate. (D) A threaded metal ring. (E) Metal plate with coordinate marks. (F) Outer ring serving as holder for the mirror. (G) Semi-translucent mirror. (H) Filling plugs.

reference for adjusting the projected coordinate system. An additional aluminum ring (Fig. 1A6, 1B3, Fig. 2F) with an inner diameter of 30 mm, an outer diameter of 38 mm and a height of 5 mm can be slid over the chamber and secured with screws at the sides. A trench in the ring allows a semi-translucent mirror (Fig. 1A8, Fig. 2G) to be adjusted at an angle of 45° to the glass and metal plate. The ring with the mirror allows one to record with the vertically mounted OI camera while projecting the coordinate grid horizontally through the semi-translucent mirror into the OIC.

2.2.4. Tube grid

The tube grid (Fig. 1A9–10, 1E, 1F) is a custom made plastic cylinder (Fig. 1A10, 1E), 15 mm in height and 17 mm in diameter. It is inserted into a hollow metal cylinder (Fig. 1A9, 1B4) which fits onto the base ring in the same way as the OIC. The metal cylinder has an opening with a fitting cover (Fig. 1A9a) at the lower front side through which the area below the plastic cylinder is accessible after insertion. A marginal notch indicated in Fig. 1F prevents the plastic cylinder from longitudinal or rotational movement within the metal cylinder. Parallel to its roll axis, the plastic cylinder contains about 3000 channels of 0.15 mm core diameter and a center to center distance of 0.22 mm.

The geometry, especially the aspect ratio of the channels, is designed to lead electrodes to their target points, i.e. the point at which the rotational axis of the channel crosses the cortex, with extreme precision and the highest resolution possible. This precision can be calculated by using the dependence of the maximum electrode displacement on the channel aspect ratio and the electrode diameter (Fig. 3):

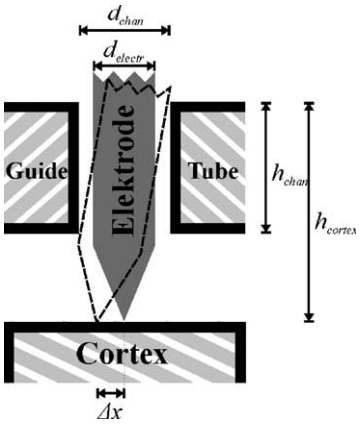

Fig. 3. Angular play of an electrode in a channel.

$$\Delta x = (d_{\text{chan}} - d_{\text{electr}})\left(\frac{h_{\text{cortex}}}{h_{\text{chan}}} - \frac{1}{2}\right)$$
$$= (0.15\ \text{mm} - 0.12\ \text{mm})\left(\frac{20\ \text{mm}}{15\ \text{mm}} - \frac{1}{2}\right) = 0.025\ \text{mm} \quad (1)$$

where Δx is the maximum distance of the electrode tip to the rotational axis of the channel, d_{chan}, the channel diameter, d_{electr}, the electrode diameter, h_{cortex}, the height of the upper end of the channel relative to the cortical surface and h_{chan}, the height (length) of the channel. The values inserted are typical for the setup we used and yield a maximum error of 0.025 mm in electrode position. Together with the uncertainty due to the resolution of the functional maps of 0.025 mm, the accuracy which can theoretically be reached with this approach is about 0.05 mm.

The tube grid was developed in cooperation with microTEC GmbH (microTEC, Gesellschaft für Mikrotechnologie, Bismarckstrasse 142b, 47057 Duisburg, Germany) using Rapid Micro Product Development (RMPD®) technology.

2.2.5. Projector

In order to determine the cortical coordinates of the optical imaging map a coordinate system has to be projected onto the cortical surface by means of a customized projection device (Fig. 4). The projection device is mounted onto an optical bench (Fig. 4A) and consists of a modified slide projector (Fig. 4B), which allows for precise translational movement in all (x, y, z) axes by use of micro-drives (Fig. 4C) and an optical lens (f = 200 mm) (Fig. 4D). Moving the slide in an x- or y-direction alters the position of the projected image, whereas a movement in the z-direction (that is parallel to the optical axis) will adjust the size to the reference size given on the metal plate (1A). The optical bench is movable (Fig. 4E) along the optical axis of the projector for adjusting the focus. It is mounted on a knuckle joint

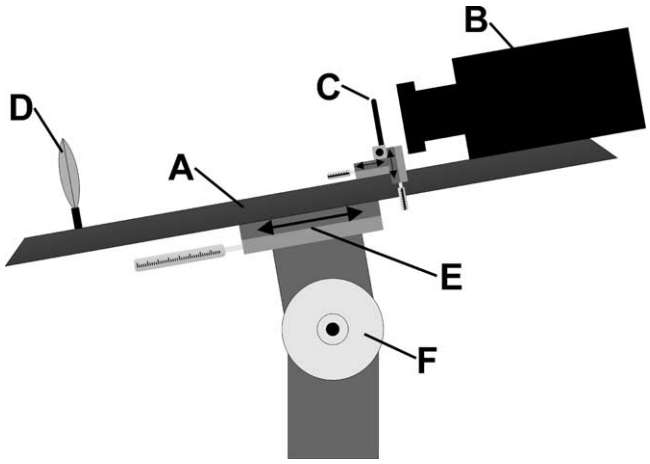

Fig. 4. The projection device. (A) Slide projector without any slide inserted. (B) The slide of the coordinate grid mounted onto a *xyz*-axis stage. (C) Optical lens with a focal distance of 200 mm. (D) Optical bench. (E) Linear micro-drive stage which moves the whole optical bench. (F) Knuckle joint.

(Fig. 4F) to adjust the angle of the projector in the plane of the optical axis and the optical bench, i.e. vertically.

2.2.6. Manipulator

The manipulator (Fig. 5) is a custom made device to move the electrodes back and forth. It consists of 16 linear micro-drives (Fig. 5 inset A) which can be moved at high precision. In order to minimize the spacing, the micro-drive movements are transmitted through Bowden cables which converge onto a suspension (Fig. 5 inset B1) confining them to an area of 14×6 mm. Electrodes are attached to the endings of the inner Bowden cables. These connections are established by insulating the end parts of the inner Bowden cables with Teflon sockets (Fig. 5 inset B2), plugging small metal tubes (Fig. 5 inset B3) into the Teflon sockets and sticking the bent end parts of the electrodes into the metal tubes. The tension of the bent electrode end parts presses the electrode wires against the inner walls of the metal tubes, thus connecting them mechanically to the Bowden cable movements and electrically to the metal tubes. The metal tubes, in turn, are connected by thin wires (Fig. 5 inset B4) to the pre-amplifyers. To further reduce the spacing between the electrodes they are funneled through guide tubes (Fig. 5 inset B6) which depart from an area of 14×6 mm (Fig. 5 inset B5) onto an area of 8×4 mm (Fig. 5 inset B7). Some centimeters below, the metal cylinder (Fig. 5 inset B9) containing the tube grid (Fig. 5 inset B8) is attached to the manipulator to guarantee a fixed distance between the tube grid and the Bowden cable suspension.

2.3. Animal preparation

Animal experiments were performed on cat visual cortical area 18. Anesthesia was initiated by intramuscular injection of ketamine hydrochlorid (10 mg/kg, Ketamin, CEVA Tiergesundheit GmbH, Düsseldorf, Germany) and xylazine hydrochlorid (2.5 mg/kg, Rompun, BayerVital, Leverkusen, Germany) and maintained after tracheotomy by artificial ventilation with a mixture of N_2O (70%), O_2 (30%) and halothane (0.5–1.0%, Halotan, Eurim-Pharm Arzneimittel GmbH, Piding, Germany). The cat's head was fixed by mounting the head holder to the stereotactic frame and cementing the rippled bolt of the head holder to the cat's skull. Subsequently, a round craniotomy, 20 mm in diameter was performed over occipital cortex centered on A2/L0 according to Reinoso-Suarez (1961). The base ring was placed concentrically over the craniotomy and cemented onto the skull (Fig. 1C). During this procedure, the threaded holes in the base ring were temporarily closed with screws in order to prevent the cement to enter. After surgical procedures had been terminated, a systemic muscle relaxant (pancuronium, 0.3 mg/kg per h, Pancuronium, CuraMED Pharma GmbH, Karlsruhe, Germany) was administered intravenously to prevent eye movements during optical and electrophysiological recordings. All animal experiments were performed in accordance with the guidelines for the use of animals in research of the Society for Neuroscience and the German law for the protection of animals.

2.4. Optical imaging

Optical imaging was performed using standard techniques as described previously (Bonhoeffer and Grinvald, 1993). After fixation of the base ring, the OIC (Fig. 1A2, 1B2, Fig. 2A) was mounted onto the base ring and sealed with wax. Subsequently, the dura mater was removed over the targeted hemisphere. The chamber was filled with silicone oil and closed with a transparent glass plate. Changes in the optical properties of the neuronal tissue were recorded with a commercial optical imaging system (ora2001, Optical Imaging Europe, Munich, Germany) under illumination with light of a wavelength of 620 nm. The optical imaging camera was fitted with a lens system consisting of two 50 mm Nikon objectives and a $2\times$ extender providing a 3.6×4.8 mm field of view (Ratzlaff and Grinvald, 1991) at a resolution of 192×144 pixels. Visual stimuli were presented by means of either a 21″ CRT computer screen (Hitachi, CM815ET Plus, refresh rate 100 Hz) or a projection on the reverse side of a silver screen using a CCD projector (Sony, VPL-PX30, refresh rate 60 Hz) at a distance of 570 mm. Two partially overlapping maps of orientation preference were obtained by OI evoked by whole-field, high contrast square wave gratings with a

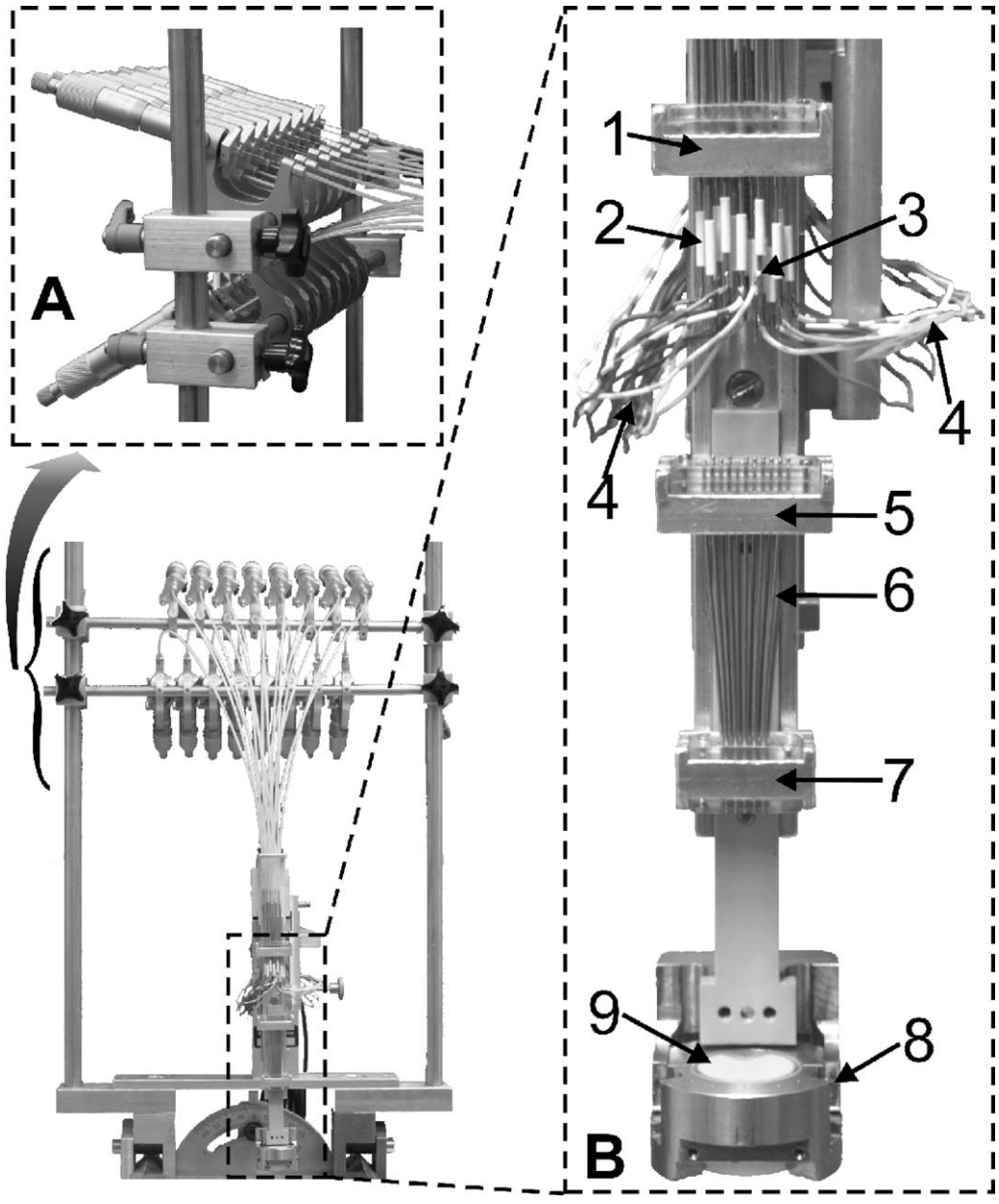

Fig. 5. The electrode manipulator. At the top, 16 micro-drives are arranged in two rows (enlarged side view in inset A). The micro-drive movements are conveyed by Bowden cables which converge to a set geometry with closer spacing (B1). The inner wires of the Bowden cables are plugged into the upper side of insulating Teflon sockets (B2), whereas metal tubes are plugged in from the lower side (B3). Cables (B4) are soldered to the metal tubes, connecting them electrically to the amplification system. Converging tubes (B6) are drawn together 20 mm beneath the soldered metal tubes. Further below, the metal cylinder (B8) holding the tube grid (B9) can be mounted onto the manipulator system.

spatial frequency of 0.15 cycles/degree moving in eight directions (0, 45, 90°, et cetera) orthogonally to the grating orientation at a velocity of 16°/s. The stimulus sequence was pseudorandomly interleaved and usually 2–4 blocks of eight repetitions for each stimulus condition were averaged. Stimuli were shown for 3 s, with an inter-stimulus interval of 7 s. Data were processed as described previously (Bonhoeffer and Grinvald, 1993) using the ''cocktail blank normalization''.

2.5. Electrophysiology

Extracellular recording of multi unit activity was performed with tungsten electrodes (average impedance ≈ 0.8 MΩ at 1 kHz, shaft diameter ≈ 120 μm, insulated with Epoxylite 6001 S, Epoxylite International Ltd., UK), which could be advanced longitudinally by means of the manipulator. The signals were amplified and band pass filtered (Butterworth, band pass from 800 to 5 kHz). Action potentials were detected by a voltage

threshold and stored as time stamps. All signals which showed clear single or multi unit activity were included in the analysis. In order to obtain direction tuning curves, visual stimulation was performed with a sinusoidal grating drifting in 12 directions with a velocity of 10°/s and a spatial frequency of 0.1 cycles/degree. Direction tunings were calculated from 20 repetitions of each stimulus condition.

2.6. Procedure for alignment of electrodes with the functional maps

After OI of two spatially slightly overlapping orientation maps, the semi-translucent mirror was mounted onto the OIC (Fig. 1A, 1D, Fig. 2). This could be done without moving the OI camera due to the flat design of the OIC. A coordinate grid was then projected through the semi-translucent mirror onto the metal plate fitted into the OIC. The projected coordinate grid was then adjusted to the coordinate marks in the metal plate and thus brought into a defined position and scale with respect to the base ring. After removing the metal plate, the whole optical bench with the projection device was advanced until the coordinate grid was focused on the cortical surface. Then, an image of the coordinate grid was taken by the OI camera, in exactly the same position as used for the recording of functional maps. This enabled us to determine the precise position of each pixel relative to the base ring. In addition, video images from the cortical surface were taken under illumination with green light to document the local blood vessel patterns. Therefore, three pairs of overlapping images existed at the end of this procedure: one pair of orientation maps, one pair of the projected coordinates and one pair of blood vessel patterns. All pairs of images covered the same cortical region of about 4×8 mm.

The second device to be placed on the base ring was the tube grid fixated in the metal cylinder (Fig. 1A9–10, 1B4, 1F). The functional maps, the images of the projected coordinates, the images of the cortical surface and the exact position of the tube grid relative to the base ring were fed into a custom made computer program. This program aligned all three pairs of images and calculated the positions of the guide tubes relative to the functional map. The guide tube positions were visualized as circles on the functional map as shown in Fig. 8B. Subsequently, the desired recording sites were selected from the available guide tube positions by mouse-clicking on the respective positions on the functional map. After the computer program had returned the row and column numbers of the corresponding guide tubes, the micro-electrodes were inserted under a microscope, by hand, backwards into the respective channels of the tube grid. The metal cylinder containing the tube grid was then attached to the manipulator chassis, so as to assure a set distance between the tube grid and the Bowden cables' initial positions. The electrodes were funneled through the converging tubes of the manipulator (Fig. 5 inset B6), clamped to the Bowden cables by removing the insulation at the end parts with a piece of sandpaper, bending the upper ends and sticking them into the narrow metal tubes at the end parts of the Bowden cables (Fig. 5 inset B3). Finally, the manipulator, including the metal cylinder with the tube grid, was placed onto the stereotactic frame. The manipulator was moved until the metal cylinder came to rest on the base ring and subsequently fixed with screws onto the base ring. The electrodes were advanced under optical control (through the opening at the front of the tube grid holder) until their tips almost touched the cortical surface. The space between the cortex and the tube grid was then filled through this opening with Agar (3% in Saline) to minimize cortical movements and to protect the cortex. At this point, the system was ready for advancing the micro-electrodes into the cortex.

2.7. Ex-vivo test of system precision

Prior to application in animal experiments, the method has been thoroughly tested for its spatial precision. The examined variable was the system's ability to guide electrodes to the desired locations as defined by the channel positions of the tube grid. This was done by carrying out the whole procedure using a thin disc of plasticine in place of a living brain and a blunt electrode wire instead of an electrode with a tip. In lieu of recording activity maps, pictures were taken from the plasticine surface and landmarks on the plasticine surface served to realign the camera position. After the blunt electrode wires had been inserted into the selected guide tubes of the tube grid, they were advanced into the plasticine, leaving holes in the surface. The center to center distance of the electrode marks relative to the intended target points was measured from an additional image of the plasticine surface taken after removal of the electrodes.

3. Results

3.1. System precision

The spatial precision with which the system guides electrodes to the selected channel targets on the feature map was determined ex-vivo as described above. The procedure for determination of the system's spatial precision was carried out seven times using several electrodes inserted into different channels in each experiment. As shown in Fig. 6, the electrodes approached the target points as close as 64 μm on average, with a maximum error of 130 μm. No systematic error in electrode placement could be detected from the direc-

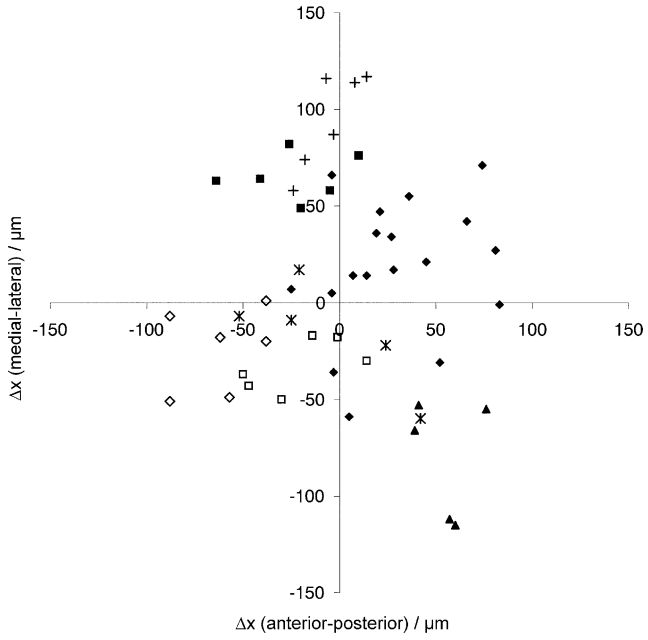

Fig. 6. Deviation of holes in the plasticine from the intended target point. Points marked with the same symbol belong to electrode wire insertions during the same experiment, but into different channels, i.e. each symbol represents one experiment. The channels chosen for insertion differ between the experiments in order to cover a large sample of channels throughout the entire tube grid.

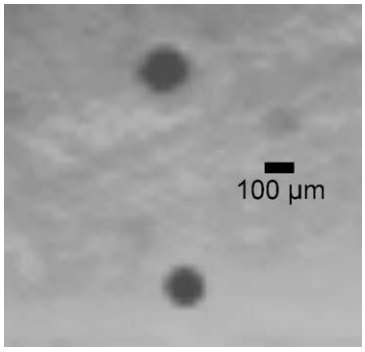

Fig. 7. Image of the plasticine surface taken by the optical imaging camera. The lower dark spot resulted from dipping an electrode once into the plasticine, the upper one resulted from several insertions through one channel of the tube grid whilst bending the end of the electrode into a different direction each time.

tions of displacement over all repetitions and electrode insertions. Comparison of the standard deviation (S.D.) of the distances to the intended target points ($\sigma =$ 30 µm) to the S.D. of the same data after vector subtraction of the center of mass within each experiment ($\sigma = 17$ µm) suggests that a major part of the deviation could be attributed to imprecise projection of the coordinates, since this error influences all electrode positions within one experiment in a common manner. The electrodes' angular play in the channels did apparently not contribute substantially to the deviations. Fig. 7 shows two holes in the plasticine. The lower one resulted from a single insertion of a blunt electrode wire through a channel, whereas the upper one resulted from ten insertions into another channel whilst inclining the wire into a different direction each time in order to fully exploit the whole range of angular play. The radius of the upper hole as measured with a calibrated microscope reticule is, at most, 20 µm greater than that of the lower one. Assuming the blunt end of the wire would widen the hole by the amount of its displacement, this indicates that the precision is of the same order of magnitude as calculated (Eq. (1)).

3.2. Animal experiment

To test whether any unpredictable effects may render the above results invalid when the system is implemented in animal experiments, we used this method for positioning several electrodes according to orientation maps in area 18 of the cat visual cortex. The time course of such an experiment is as follows: implantation of recording chamber and adjustment of optical imaging setup, 6 h; recording of optical data, 2 h; adjusting and imaging of the projected coordinates, 2 h. The time required for the selection of recording sites and the preparation of the electrode manipulator system is highly dependent on the number of electrodes to be used. Therefore, about 3–6 additional h are required until the recording setup is ready for advancing the electrodes into the cortex.

Since it is difficult to determine from histological reconstructions and superimposed functional maps the precise locations at which the electrodes had entered the cortex, we compared the direction preferences of the electrophysiological recordings with the selected target points in the feature map. Fig. 8 shows the orientation map and the direction preferences for all electrodes from which visually evoked activity was recorded. All measurements of selectivity are congruent with the expectations from the functional maps. The best correspondence exists for electrodes 2, 4 and 5 whose direction tunings exactly agree with what one would expect from the target sites of the feature map (Fig. 8B). Electrodes 1 and 3 differ slightly from the feature map such as if they hit the feature map about a hundred micrometer right below to the intended target point. In order to quantify the match, we determined the preferred orientation at an intended recording site by vectorial summation of all pixel orientations within a radius of 75 µm around the desired target point in the orientation map. This corresponds to the area under the respective guide tube as shown by circles in Fig. 8B. For the electrophysiological recordings, we classified that orientation as the preferred one that corresponds to the longest vector in the tuning curve. For electrodes

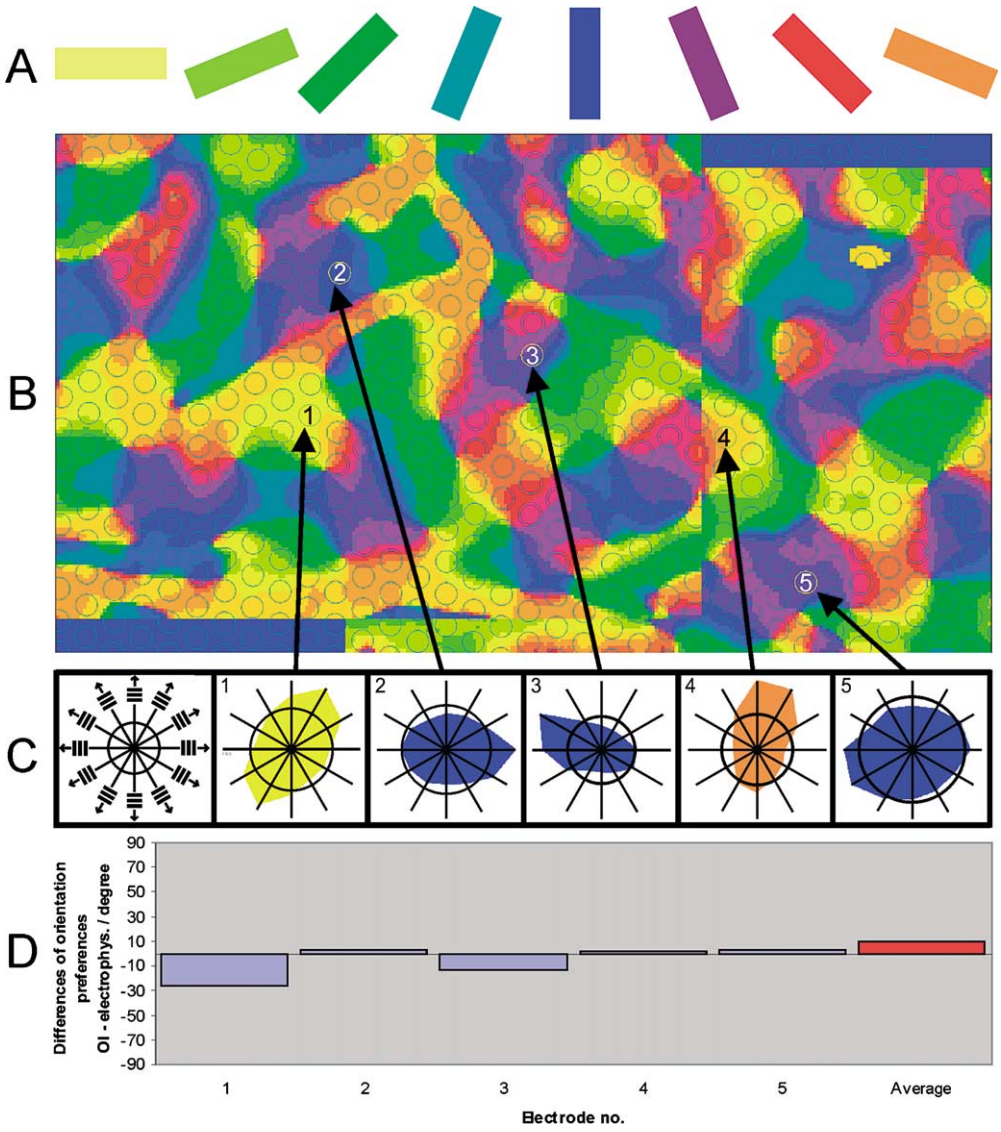

Fig. 8. Comparison of orientation preferences as determined by OI and electrophysiological recordings. (A) The colored bars relate the preferred grating orientation to the color code in the orientation map. (B) Two overlapping orientation maps aligned such that the corresponding images of the epicortical vessels would optimally fit if aligned in the same manner. (C) The polar plots labeled from 1 to 5 show the direction tunings of the multi unit activity as recorded with the respective electrodes. In the leftmost box, gratings and their drifting directions are sketched at the elongation of the corresponding polar plot axis as used for the tuning curves. Arrows point from the tuning curves in (C) to the intended recording sites in (B). (D) Differences in preferred orientation between optical and electrophysiological recordings. The rightmost beam shows the average absolute difference of all five electrodes.

2, 4 and 5, the preferred orientation differs by only 2–3° from that of the orientation map. For electrode 3, the difference amounts to 13 and for electrode 1–26°.

These values agree with the spatial deviations we anticipated from our ex-vivo experiments and indicate that the targeting method successfully placed the electrodes into the desired sites of the feature map. With up to 16 electrodes, some of them as close to each other as 660 μm, we observed neither visible cortical damage, nor did we loose the responses of cells without deliberately changing the electrode depths by the respective electrode drives. Although dimpling effects could not be observed directly due to the Agar above the cortex, the missing cross-influence between the individually adjustable electrodes suggests that no severe dimpling effects had occurred. Moreover, Fig. 9 compares two examples of the PSTHs and orientation tunings of two recording sessions separated by more than 3 h time. The similarity of these two data sets illustrates the stability of the recording conditions which allowed us to record unchanged neuronal responses over several hours throughout the experiment's duration of up to 5 days.

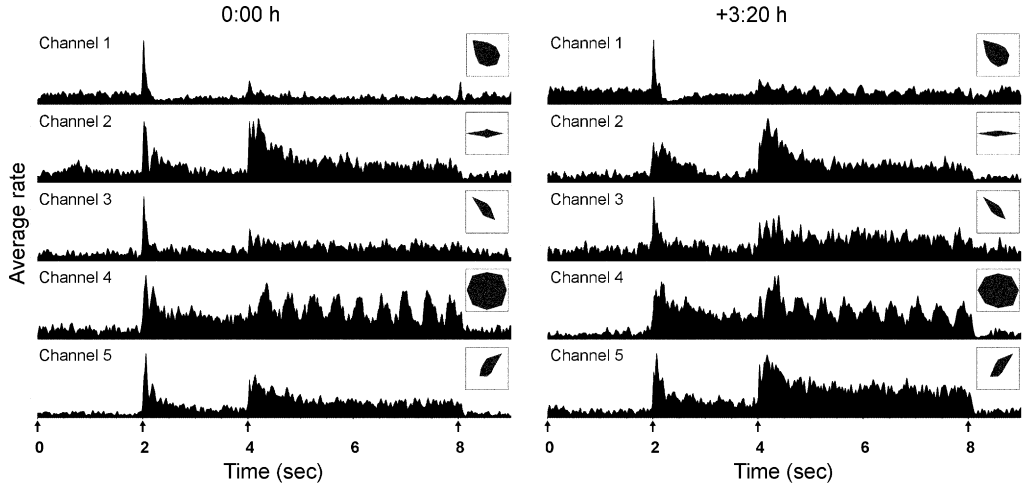

Fig. 9. PSTHs and tuning profiles (insets) of multiple unit responses recorded from five electrodes. For the PSTHs the responses were averaged over all eight different conditions of a whole field grating stimulus and smoothed with a Gaussian Kernel of 50 ms width at half height. The data in the right column were recorded 3 h 20 min later than the data of the left column. The onsets of the distinct phases of the stimulus protocol are indicated by arrows at the time axis. In the first 2 s, an iso-luminant gray screen was presented. After 2 s, a static oriented grating appeared and started to drift after another 2 s. The grating disappeared at time 8 s and the initial gray screen was shown for the last second of the protocol. The insets in the upper right corner of each PSTH show the orientation tuning of the respective channel as calculated from the same data sets.

4. Discussion

4.1. Summary

We have developed a device which allows for the targeted electrophysiological recording from single neurons at multiple preselected cortical sites in parallel. As discussed below, this method allows for free selection of quantized recording sites from overlapping functional OI maps, covering a cortical region of about 4×8 mm and for subsequent precise positioning of the electrodes to the corresponding cortical sites. Additionally, the depth of penetration remains individually adjustable for each electrode. The method is applicable to virtually all cortical areas where OI can be performed and is not restricted to the use of tungsten microelectrodes only.

4.2. Fabrication of the tube grid

The tube grid is an integral and crucial part of this new recording approach. Ideally, it should allow for recording with infinitesimal thin electrodes and individual guide tubes should have likewise infinitesimal thin walls to allow for optimal resolution in targeting the locations within the feature maps. Practically, however, its geometry, and therefore, its resolution is to great extent dictated by technical constraints such as the required diameter of an electrode to remain stable when advancing and thickness of channel walls to ensure stability of the material. Moreover, the aspect ratio of the channels should be as high as possible in order to minimize the angular play of the electrodes and, by this, optimize the system precision; the spacing between the channels should be as small as possible to result in the highest possible system resolution. In addition, the material should be elastic, for the thin walls between the channels must not break or damage the electrode's insulation. Finally, the material must be inert under exposure to a humid environment and cerebrospinal fluid because this would alter the channel positions and could immobilize the electrodes within the channels.

Conventional product engineering approaches such as drilling or etching proved to be unsuitable. Our solution was to develop such a tube grid in cooperation with a company (microTEC) mastering the RMPD® technology. With this technology it is possible to build up the tube grid by binding a liquid monomer layer after layer by masked light rays. By just altering the light mask other geometries can easily be produced.

The final product, the tube grid, possesses the requirements stated above: the material is insulating, elastic and it did not swell when sunk into pure water over 2 weeks time; the channels have an extremely high aspect ratio of 15.0: 0.15, being crucial to the system precision by leaving very little angular play to the electrodes; the precision of RMPD® and the elastic material made it possible to produce channels of a diameter just above the electrode's diameter and walls between the channels as thin as 0.07 mm resulting in a high system resolution. Further improvements of the system's resolution by optimizing electrode diameter and channel wall thickness may well be possible and the final limitation of this approach in terms of practical resolution has not yet been reached.

Furthermore, we are confident that the flexibility, rapidity and low cost of RMPD® production allows for the fast construction of similar tube grids permitting

other new approaches, inventions or techniques than the targeting method presented here.

4.3. System precision and handling

The results of ex-vivo and in-vivo measurements of the system's precision demonstrate that it is possible to simultaneously record from multiple pre-selected sites whose location is constrained only by the spacing of the tube grid channels. They further show that the system reproducibly places the electrodes with a spatial precision in the order of 100 μm relative to the determined channel position. The close spacing of the channels makes that the system's resolution suffices for most applications, i.e. the available recording sites permit to record neurons exhibiting virtually all conceivable feature constellations. Restrictions emerge only if parallel recordings are desired from structures which are smaller than the channel spacing, and therefore, smaller than the system's resolution. The number of electrodes which can be inserted with this method is only restricted by the layout of the manipulator used to advance the electrodes and, of course, by the number of channels in the tube grid (≈ 3000).

The most critical issues of the procedure are the matching of the channel positions with the feature map and the projection of the coordinate system onto the cortex. The preparation time of 14–16 h allows the performance of classical electrophysiological experiments with the added benefit of being able to implement the targeting technique. Although, we have not tested the system in a semi-chronical preparation, this should be feasible because feature maps in visual cortex are stable over time (Shtoyerman et al., 2000). Once the base ring is implanted and all necessary images are taken, the respective electrode constellations can be designated beforehand and different combinations of recording sites can be selected in different recording sessions without the need to repeat the mapping of the channel positions onto the OI map. However, the spatial relationship between base ring and cortex must not be corrupted, for instance, by actions of the behaving animal or growth of the skull.

As our ex-vivo results show, the establishment of relations between the cortical maps and the coordinate system is the most critical step with respect to the system precision. Our analysis of the inter-experimental variability indicates that errors in the position of the coordinate grid affect the mapping of all channel positions onto the functional map in a common manner and thus introduces a systematic error in the resulting electrode positions (which can lead to unsystematic errors in neuronal feature response due to the inhomogeneous organization of the feature map). This variability is greater among the experiments than within one experiment. We have realized the match between maps and electrode positions by projecting the coordinate system directly onto the cortical surface. This is superior to the use of a coordinate system which is positioned, e.g. on a glass plate, above the cortex because the distance of the plate to parts of the curved cortical surface is never constant and hence errors due to parallactic distortions are unavoidable. Errors associated with the direct projection of the coordinate grid onto the cortical surface could arise from inhomogeneous refraction and reflection due to the curved moist surface of the cortex. These problems have been overcome by projecting the coordinate grid through the liquid filled OIC that was closed with a glass plate and provided a plane transition from air to the fluid.

Another potential problem is dimpling: the electrodes, although very thin and sharp, depress the cortical tissue. This dimpling effect increases with the number of electrodes used and can influence neuronal activity or even damage the cortex. Dimpling also affects the stability of the recording, since the elastic cortical tissue will slowly return to its initial position, which virtually has the same effect as advancing the electrodes deeper into the cortex. Even though our method does not avoid these problems, the targeted positioning of the electrodes reduces the number of electrodes required to record cells with the desired properties and, thus, minimizes dimpling and potential cortical damage.

4.4. Alternative approaches

Some approaches for the placement of multiple electrodes according to functional maps have been published. However, these lack several of the advantages of our method such as individual electrode adjustability or the freedom of targeting multiple cortical sites independently as outlined in greater detail below. Other approaches like a recently described device (Arieli and Grinvald, 2002) are optimized for different purposes such as the simultaneous recording of OI data together with electrophysiological data from one or a few electrodes and are thus not comparable to our technique.

One of the most common techniques for advancing multiple electrodes into a relatively confined cortical region uses arrays of guide tubes. The guide tubes are mounted onto a holder which allows them to be arranged in a fixed geometric constellation. The electrodes are guided through the tubes to their target points, which in turn can only be altered collectively by moving the holder of the guide tubes. In principle, it should be possible to enhance the chance of recording a desired combination of neuronal response properties with the different electrodes by fitting the design of the guide tube holder to typical columnar distances. After the OI feature maps have been obtained, this module could be positioned by using the pattern of epicortical blood

vessels on the cortical surface as a spatial reference. The success of this approach, however, depends on the regularity of the functional organization, which, in turn, is highly dependent on the feature to be mapped by OI (Hübener et al., 1997), the species (Rao et al., 1997), the individual animal (Horton and Hocking, 1996), the cortical area (compare Bonhoeffer and Grinvald, 1991; Rao et al., 1997) and the spatial extent of the electrode insertion sites. Therefore, the limited regularity of cortical domains will not allow for an optimal positioning of the electrodes when separated by up to several millimeters.

Another technique of recording from previously characterized regions is to use thin wires that are chronically implanted into the cortex as described by Mioche and Singer (1988). This method has the advantage of allowing for the unconstrained placement of several electrodes. As for the fixed guide tube design, the positioning of the electrodes is accomplished by visual orientation along the pattern of epicortical blood vessels. This method has proven to be sufficiently accurate to target selected orientation domains in cat primary visual cortex (Galuske et al., 1997; Schmidt et al., 2001). It is suited for parallel optical and electrophysiological recordings and for recordings in behaving animals. However, it lacks the possibility of manipulating the penetration depth of electrodes after they have been implanted into the cortex. Furthermore, the electrode density is restricted due to the glue around each electrode which is needed to fix the electrodes after insertion.

In summary, the techniques available for the precise placement of multiple electrodes according to functional maps constrain either the possibility to independently select many different recording sites or to advance the electrodes once they are positioned. An ideal solution would consist e.g. of an array of extremely small and maybe even implantable micro-drives put together to a device which renders both possible, the precise placement of electrodes and the possibility to advance them. For the time being these drives and devices are not available. Therefore, the new method we present here combines the advantages of the available methods. By using the tube grid the idea of guide tubes with a fixed geometry is maintained but the necessity of moving electrodes or guide tubes to a certain site above the cortex is avoided. The main improvement over common guide tubes is the extremely high aspect ratio of the channels which has two advantages: first, the electrodes are guided very precisely to their target points and second, the channels are thin enough to be clustered together forming a matrix of densely packed guide tubes. These improvements allow for new possibilities, as the absolute and the relative electrode positions can be defined ad hoc without building a new guide tube holder. Furthermore, the precise parallel guidance of the electrodes allows for accurate definition of electrode spacing as well as for high density arrangements. Adding the possibility of mapping the channels positions onto a functional OI map as we outlined in Section 2 allows for a choice from hundreds of possible recording sites with defined functional properties as determined by OI. We thus consider our method to be a good compromise between technical complexity and the experimental need of unrestricted, independent and precise placement of several electrodes according to functional OI maps.

5. Conclusion

Given the precision with which the system is able to guide the electrodes to target points segregated by distances in the centimeter range, a large variety of applications in brain research could be envisaged: investigation of interactions between local peculiarities in feature representations (e.g. singularities and fractures in visual cortex) and identified domains within areas as well as between topographically corresponding regions in different areas or hemispheres. Moreover, the device is not restricted to a certain geometry of the applied probes except for their diameter. Thus, incorporating a tool for front-loading the tube grid with probes, combined recording, stimulation and pharmacological application at predefined sites using single electrodes, tetrodes or pipettes is conceivable. In summary, we consider this novel method ideally suited for studying complex interactions between multiple functionally defined sites using multi electrode recordings, multi site stimulation or pharmacological manipulations.

Acknowledgements

We would like to thank Sandra Schwegmann for her outstanding technical assistance during the experiments, Sergio Neuenschwander for providing data acquisition and analysis systems, Walter Ankenbrand, Thomas Maurer and Andreas Umminger for their advice, discussions and the preparation of the mechanical devices.

References

Arieli A, Grinvald A. Optical imaging combined with targeted electrical recordings, microstimulation, or tracer injections. J Neurosci Methods 2002;116:15–28.

Bonhoeffer T, Grinvald A. Iso-orientation domains in cat visual cortex are arranged in pinwheel- like patterns. Nature 1991;353:429–31.

Bonhoeffer T, Grinvald A. The layout of iso-orientation domains in area 18 of cat visual cortex: optical imaging reveals a pinwheel-like organization. J Neurosci 1993;13:4157–80.

Bonhoeffer T, Grinvald A. Optical imaging based on intrinsic signals. In: Toga AW, Mazziotta JC, editors. Brain Mapping: the Methods. San Diego: Academic Press, 1996:55–97.

Engel AK, Fries P, Singer W. Dynamic predictions: oscillations and synchrony in top–down processing. Nat Rev Neurosci 2001;2:704–16.

Galuske RAW, Singer W, Munk MHJ. Reticular activation facilitates use-dependent plasticity of orientation preference maps in the cat visual cortex. Soc Neurosci Abstr 1997;23:2059.

Gelnar PA, Krauss BR, Szeverenyi NM, Apkarian AV. Fingertip representation in the human somatosensory cortex: an fMRI study. Neuroimage 1998;7:261–83.

Gilbert CD, Wiesel TN. Clustered intrinsic connections in cat visual cortex. J Neurosci 1983;3:1116–33.

Gilbert CD, Wiesel TN. Columnar specificity of intrinsic horizontal and corticocortical connections in cat visual cortex. J Neurosci 1989;9:2432–42.

Horton JC, Hocking DR. Intrinsic variability of ocular dominance column periodicity in normal macaque monkeys. J Neurosci 1996;16:7228–39.

Hubel DH, Wiesel TN. Receptive fields, binocular interaction and functional architecture in the cat's visual cortex. J Physiol 1962;160:107–54.

Hubel DH, Wiesel TN, Stryker MP. Orientation columns in macaque monkey visual cortex demonstrated by the 2-deoxyglucose autoradiographic technique. Nature 1977;269:328–30.

Hübener M, Shoham D, Grinvald A, Bonhoeffer T. Spatial relationships among three columnar systems in cat area 17. J Neurosci 1997;17:9270–84.

Jones EG, Coulter JD, Hendry SH. Intracortical connectivity of architectonic fields in the somatic sensory, motor and parietal cortex of monkeys. J Comp Neurol 1978;181:291–347.

Kisvarday ZF, Toth E, Rausch M, Eysel UT. Orientation-specific relationship between populations of excitatory and inhibitory lateral connections in the visual cortex of the cat. Cereb Cortex 1997;7:605–18.

Merzenich MM, Knight PL, Roth GL. Representation of cochlea within primary auditory cortex in the cat. J Neurophysiol 1975;38:231–49.

Mioche L, Singer W. Long-term recordings and receptive field measurements from single units of the visual cortex of awake unrestrained kittens. J Neurosci Methods 1988;26:83–94.

Rao SC, Toth LJ, Sur M. Optically imaged maps of orientation preference in primary visual cortex of cats and ferrets. J Comp Neurol 1997;387:358–70.

Ratzlaff EH, Grinvald A. A tandem-lens epifluorescence macroscope: hundred-fold brightness advantage for wide-field imaging. J Neurosci Methods 1991;36:127–37.

Reinoso-Suarez F. Topographischer Hirnatlas der Katze, 1 ed. Darmstadt: E. Merck AG, 1961.

Reppas JB, Niyogi S, Dale AM, Sereno MI, Tootell RB. Representation of motion boundaries in retinotopic human visual cortical areas. Nature 1997;388:175–9.

Ruben J, Schwiemann J, Deuchert M, Meyer R, Krause T, Curio G, Villringer K, Kurth R, Villringer A. Somatotopic organization of human secondary somatosensory cortex. Cereb Cortex 2001;11:463–73.

Salinas E, Sejnowski TJ. Correlated neuronal activity and the flow of neural information. Nat Rev Neurosci 2001;2:539–50.

Schmidt KE, Löwel S. Long-range intrinsic connections in cat primary visual cortex. In: Payne BR, Peters A, editors. The Cat Primary Visual Cortex. San Diego: Academic Press, 2002:387–426.

Schmidt KE, Grün S, Singer W, Galuske RAW. Parallel multi-unit recordings in primary visual cortex of the unrestrained awake and sleeping cat. Soc Neurosci Abstr 2001;27:821.58.

Shtoyerman E, Arieli A, Slovin H, Vanzetta I, Grinvald A. Long-term optical imaging and spectroscopy reveal mechanisms underlying the intrinsic signal and stability of cortical maps in V1 of behaving monkeys. J Neurosci 2000;20:8111–21.

Tusa RJ, Palmer LA, Rosenquist AC. The retinotopic organization of area 17 (striate cortex) in the cat. J Comp Neurol 1978;177:213–35.

Tusa RJ, Rosenquist AC, Palmer LA. Retinotopic organization of areas 18 and 19 in the cat. J Comp Neurol 1979;185:657–78.